Available online at www.sciencedirect.com
ScienceDirect
Journal of the European Ceramic Society 31 (2011) 1997–2004
www.elsevier.com/locate/jeurceramsoc

Influence of hydrothermal synthesis conditions on BNT-based piezoceramics

Jean-François Trelcat *, Sophie d'Astorg, Christian Courtois, Philippe Champagne, Mohamed Rguiti, Anne Leriche

Laboratoire des Matériaux Céramiques et Procédés Associés, EA 2443, Université de Lille Nord de France, PECMA Z.I. Champ de l'Abbesse, 59600 Maubeuge, France

Received 7 January 2011; received in revised form 6 April 2011; accepted 17 April 2011
Available online 13 May 2011

Abstract

The $Bi_{0.5}Na_{0.5}TiO_3$ perovskite (BNT) is a very promising lead-free candidate for piezoelectric applications. Nevertheless a low reproducibility is commonly reported for the solid state synthesized BNT. In this work, the hydrothermal synthesis was investigated to improve the BNT ceramics characteristics reproducibility. The synthesis conditions were studied in order to control more particularly the BNT grain size, crystallinity and stoichiometry.

Thanks to the slow hydrolysis of titanium isopropoxide with bismuth nitrate pentahydrate, well crystallized BNT-based powder was synthesized at 265 °C. Nevertheless this powder exhibited secondary amorphous phases. Such secondary phases synthesis was limited and prevented by both lowering the temperature synthesis down to 160 °C and optimizing the washing conditions of the powder. The BNT was finally made free of any amorphous phase by using a hydrochloric solution. The BNT sinterability was improved and BNT-based piezoceramics exhibiting a d_{33} as high as 60 pC/N were successfully produced.

Keywords: Hydrothermal synthesis; BNT; Lead-free; Electrical properties; Piezoelectric properties

1. Introduction

Lead-based piezoelectric ceramics in a perovskite like structure ($Pb(Zr,Ti)O_3$) present the most interesting piezoelectric properties near the morphotropic phase boundary and are used in many electronic and ultrasonic applications (sensors, actuators, transformers[1–3]). However, due to the effects of lead toxicity, considerable efforts were made recently to develop lead-free piezoelectric ceramics. According to 2002/95/EC and 2002/96/EC directives,[4] the exclusion of electronic parts including Pb-based compounds is restricted gradually and will be prohibited in a near future.

Unfortunately, alternative lead free materials do not exhibit the same piezoelectric characteristics as the PZT ones. Numerous works turn towards new promising lead free materials to improve their piezoelectric properties in order to progressively replace PZT in piezoelectric devices. The most studied materials are $KNbO_3$, $K_xNa_{1-x}NbO_3$, $LiNbO_3$, $LiNa_{1-x}NbO_3$, $Bi_{0.5}Na_{0.5}TiO_3$-based systems.[5]

In terms of piezoelectric properties, BNT based ceramics have been reported to be interesting[6] but difficulties to obtain homogeneous and reproducible BNT powders were also reported.[7,8] To improve the powders characteristics, hydrothermal synthesis route has been investigated by Jing et al.[9] and Ma et al.[10] Nevertheless, piezoelectric properties of hydrothermally synthesized BNT piezoceramics have not been yet reported.

This study is focused on the influence of hydrothermal synthesis conditions on the piezoelectric properties of BNT ceramics. More precisely, the washing conditions were investigated to get pure BNT powder in order to improve its sinterability. The ceramics are characterized in terms of piezoelectricity. The piezoelectric properties of the as-obtained ceramics are correlated to the microstructure, the crystallinity and the chemical composition.

* Corresponding author.
E-mail addresses: jeanfrancois_trelcat@yahoo.fr, Jean-Francois.Trelcat@umons.ac.be (J.-F. Trelcat).

0955-2219/$ – see front matter © 2011 Elsevier Ltd. All rights reserved.
doi:10.1016/j.jeurceramsoc.2011.04.025

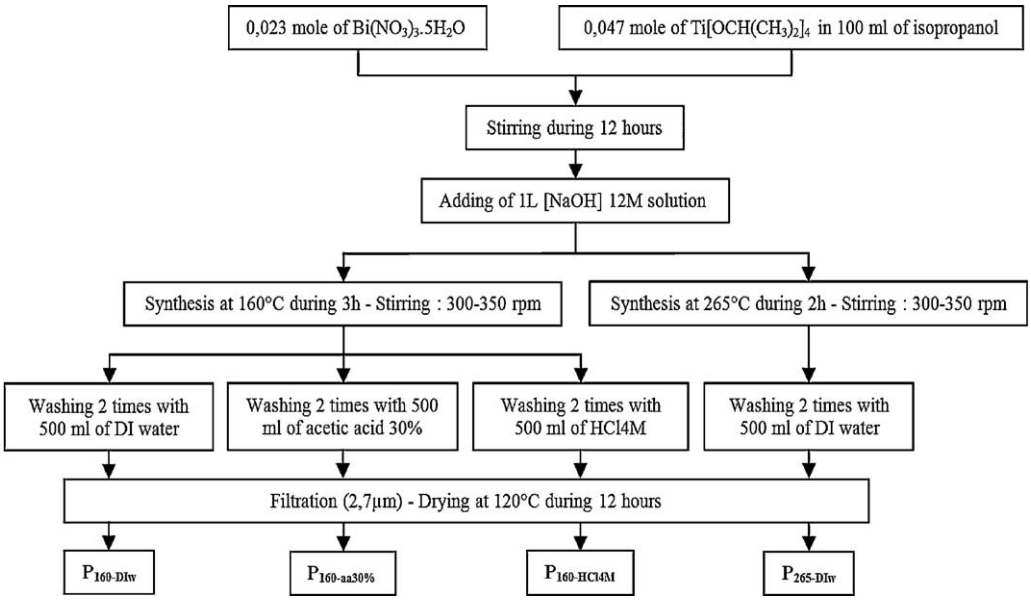

Fig. 1. Hydrothermal synthesis protocol of $P_{160\text{-DIw}}$, $P_{160\text{-aa30\%}}$, $P_{160\text{-HCl4M}}$ and $P_{265\text{-DIw}}$.

2. Experimental procedures

2.1. Hydrothermal synthesis

A flow chart illustrating the overall hydrothermal process of BNT synthesis is shown in Fig. 1. The precursors are bismuth (III) nitrate pentahydrate $Bi(NO_3)_3{\cdot}5H_2O$ and titanium (IV) isopropoxide $Ti[OCH(CH_3)_2]_4$ with purity equal to respectively 98 and 97 wt% (Sigma–Aldrich). Due to the difficult solubilization of bismuth nitrate pentahydrate, it was decided to follow the protocol of Jing et al.,[9] consisting in a mixture of both precursors $Bi(NO_3)_3{\cdot}5H_2O$, $Ti[OCH(CH_3)_2]_4$ and NaOH playing the dual role of mineralizer and sodium precursor. The hydrothermal synthesis conditions were assumed to be enough aggressive to make the bismuth nitrate totally dissolved. Starting with 0.047 mole of titanium with a Bi/Ti ratio of 0.5 and taking into account the respective impurities of $Bi(NO_3)_3{\cdot}5H_2O$ and $Ti[OCH(CH_3)_2]_4$, titanium isopropoxide in 100 ml of isopropanol solution and bismuth nitrate pentahydrate are mixed together during 12 h. Before hydrothermal treatment, 1 L of NaOH 12 M is added to the previously prepared Bi–Ti mixture. The hydrothermal reactions were carried out in a 3 L zirconium-lined autoclave.

Two kinds of synthesis were performed: the first one at high temperature (265 °C for 2 h), the second one at low temperature (160 °C for 3 h). The powders named $P_{160\text{-DIw}}$ and $P_{265\text{-DIw}}$ were washed two times with 500 ml of DI water, filtered and dried at 120 °C for 15 h.

2.2. Washing conditions

Three washing conditions were investigated for the 160 °C hydrothermally synthesized powders: DI water; 30% acetic acid solution; hydrochloric acid solution (4 M). These powders are respectively named: $P_{160\text{-DIw}}$, $P_{160\text{-aa30\%}}$ and $P_{160\text{-HCL4M}}$.

2.3. Powder characterizations

Powder size distribution was investigated by laser diffraction particle size analyser (Malvern Mastersizer 2000) with a previous dispersion of powders in DI water. The BNT powder structure was determined by an X-ray diffractometer (Rigaku Miniflex). The analysis was performed in the range 20–90° 2θ. The morphology and EDX mapping of the BNT particles were determined by scanning electron microscopy (Hitachi S-3500N).

2.4. Ceramic elaboration

After drying, powders were sieved to 40 µm and then shaped by isostatic pressing (3000 bar). The ceramics were sintered at

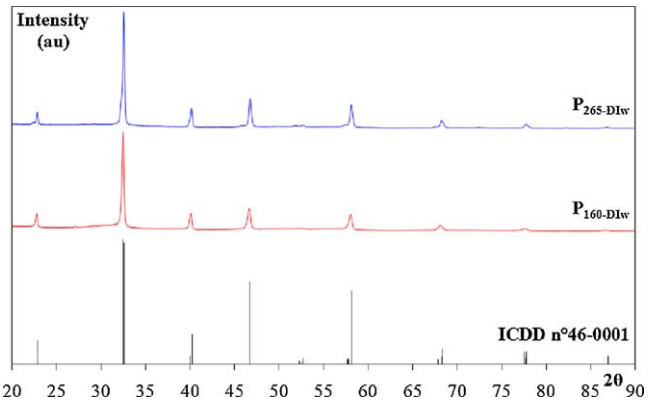

Fig. 2. XRD patterns of ICDD file no. 46-0001, $P_{160\text{-DIw}}$ and $P_{265\text{-DIw}}$.

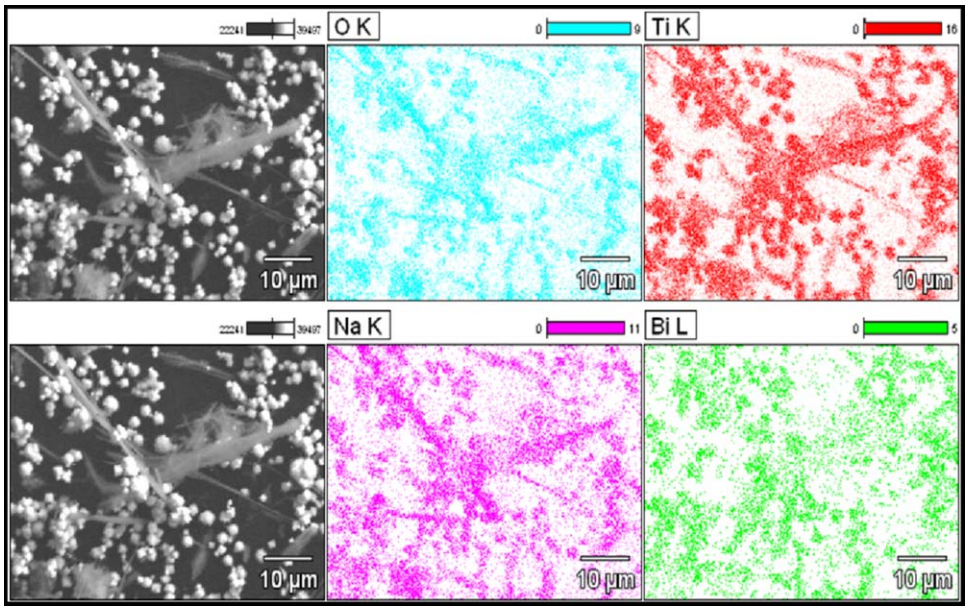

Fig. 3. EDX mapping of acicular grains observed on $P_{265\text{-}DIw}$.

1050 °C or 1150 °C for 4 h in air, in BNT powder obtained by conventional solid state route. The as-prepared samples are 5 mm in diameter and 0.5 mm in thickness.

2.5. Ceramic properties

The microstructure and EDX mapping were observed by scanning electron microscopy (Hitachi S-3500N). For electrical measurement, silver electrodes were deposited by screen printing on each face. The silver paste was dried at 150 °C during 15 min and fired at 650 °C during 5 min. A 6 kV mm^{-1} electric field was applied for ceramic polarization. The polarization step was operated in an oil bath heated to 60 °C during 1 h. A piezometer (PIEZOTEST, Piezometer system PM200) was used to measure the d_{33} charge constant.

3. Results and discussion

3.1. Influence of temperature

The XRD patterns of $P_{160\text{-}DIw}$ and $P_{265\text{-}DIw}$ (Fig. 2) show that single phased BNT powders were obtained at 160 and 265 °C. All diffraction peaks are assigned to the BNT structure as reported in ICDD file no. 46-0001, showing that the synthesized particles were single phased BNT. Nevertheless, a synthesis temperature of 265 °C ($P_{265\text{-}DIw}$) seems to favor the emergence of acicular grains (Fig. 3), whereas it was not observed by Jing et al.[9] who had performed the synthesis between 180 and 220 °C.

Fig. 3 shows an EDX mapping of these acicular grains indicating the presence of Ti, O and Na. Kasuga[11] have shown that it was possible to synthesize nanotubes of TiO_2 by hydrothermal treatment of TiO_2 rutile in highly alkaline environment. Starting with 0.15 mole of nanometric rutile TiO_2 and NaOH concentration of 10 M, these nanotubes were synthesized by hydrothermal treatment at 110 °C for 20 h. During this treatment,

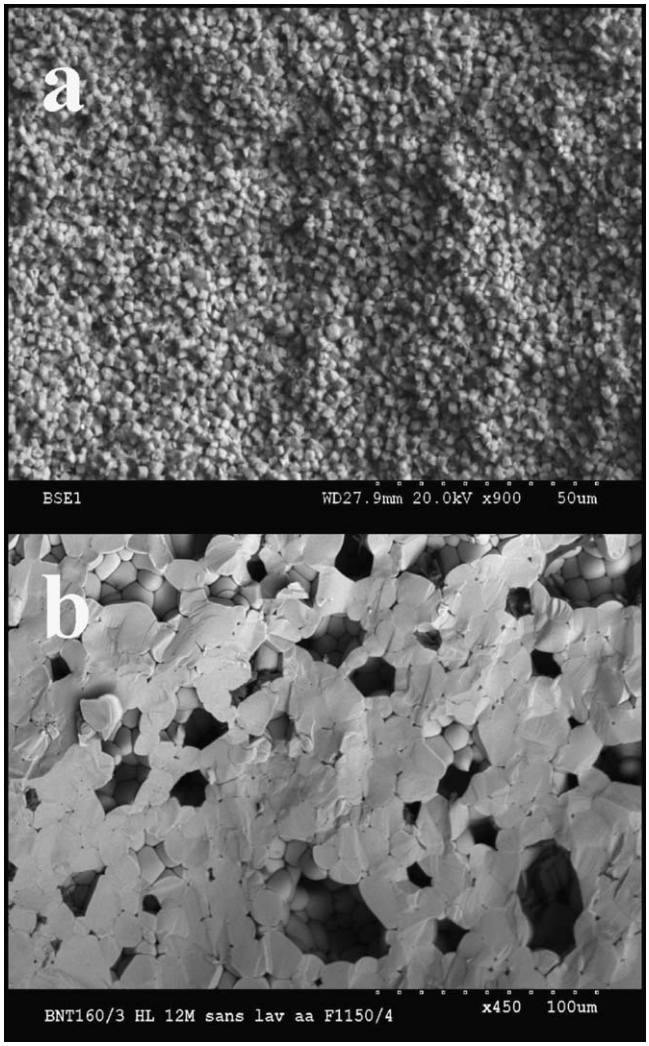

Fig. 4. SEM micrographs of the $P_{160\text{-}DIw}$ green compact (a) and sintered $P_{160\text{-}DIw}$ ceramic at 1150 °C during 4 h (b).

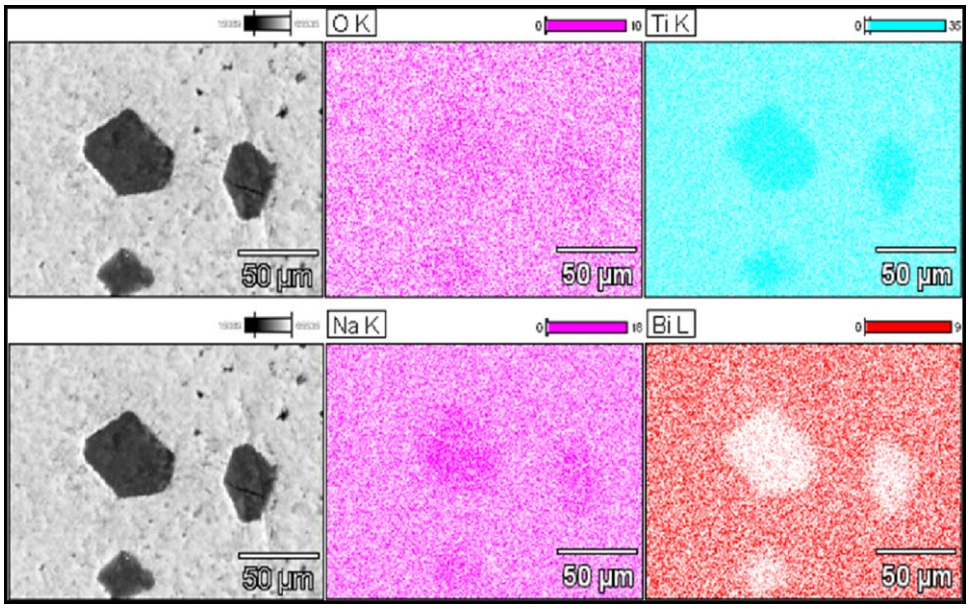

Fig. 5. EDX mapping of the 700 °C thermally treated $P_{160\text{-}DIw}$.

the Ti−O bonds break and new connections such as Ti−O−Na and Ti−OH are randomly formed explaining the presence of Na^+ ions within these nanotubes. So, these acicular grains observed in the present work are likely composed of Na-rich TiO_2. These secondary phases were not observed in Fig. 2 suggesting that these acicular grains precipitate in very limited amount and/or are amorphous.

Due to the presence of acicular grains on $P_{265\text{-}DIw}$, only $P_{160\text{-}DIw}$ powder was sintered at 1150 °C during 4 h. Fig. 4 shows the SEM micrograph of $P_{160\text{-}DIw}$ green compact and sintered $P_{160\text{-}DIw}$ ceramic.

A macroporosity (with a maximum size of 50 μm) is observed and cannot be attributed to some lack of compaction as verified on green compact micrograph (Fig. 4a) exhibiting appearance of homogeneous cluster. In order to explain such macroporosity, it was decided to treat thermally the compact at low temperature (700 °C during 4 h), to observe a possible liquid phase formation. Fig. 5 shows an EDX mapping of the as-treated $P_{160\text{-}DIw}$ compact.

Na- and Ti-rich areas can be detected by EDX and an eutectic composition seems to appear around 700 °C. The macroporosity observed at 1150 °C could be created by the sublimation of this eutectic composition at higher temperature. In the system Na_2CO_3–Na_2O,[12] an eutectic composition exist at 695 °C (27 wt% Na_2CO_3). The presence of a small amount of Na_2CO_3–Na_2O can be easily expected in the green compact

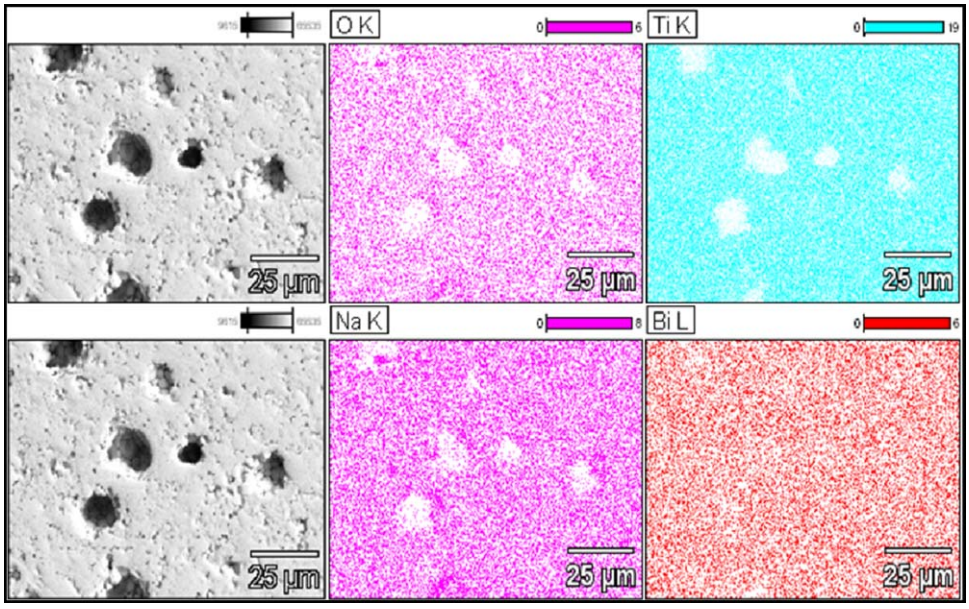

Fig. 6. EDX mapping of the 1000 °C sintered $P_{160\text{-}DIw}$.

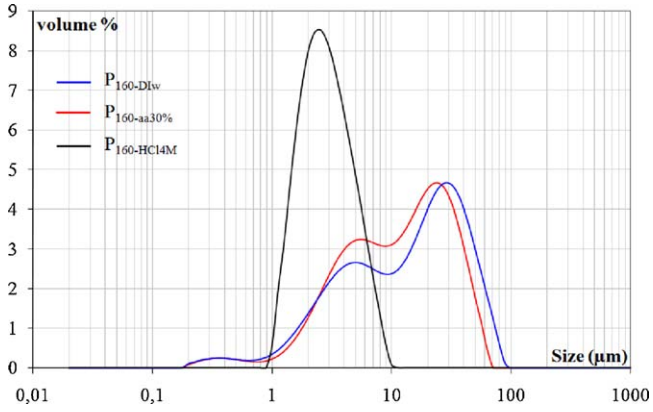

Fig. 7. Size distribution of $P_{160\text{-DIw}}$, $P_{160\text{-aa30\%}}$ and $P_{160\text{-HCL4M}}$.

(due to the large excess of NaOH) which constitutes an explanation for the eutectic formation. Another thermal treatment was performed at 1000 °C in order to explain the macroporosity formation. Fig. 6 shows an EDX mapping of $P_{160\text{-DIw}}$ sample sintered at 1000 °C. It is observed that the Na- and Ti-rich areas disappeared from the ceramic in comparison with the previous one, making the eutectic formation responsible for the macroporosity.

3.2. Influence of washing

In order to prevent the eutectic formation and then the macroporosity, two kinds of powder washing were investigated to remove amorphous phases from the powders. The first one was performed with acetic acid whereas the second one was performed with hydrochloric acid.

3.2.1. With an acetic acid 30% solution

Figs. 7 and 8 show the size distribution and SEM micrographs of the three powders $P_{160\text{-DIw}}$, $P_{160\text{-aa30\%}}$ and $P_{160\text{-HCl4M}}$ respectively. No significant size distribution evolution can be observed between DI water and acetic acid 30% washed powders except a light increase of fine particle contents (1–10 μm) and a partial deaggregation of aggregates (20–30 μm) in the case of $P_{160\text{-aa30\%}}$. Both $P_{160\text{-DIw}}$ and $P_{160\text{-aa30\%}}$ powders exhibit a cubic morphology with amorphous phases in various quantities (Fig. 8a and b).

The SEM micrograph of the sintered $P_{160\text{-aa30\%}}$ piezoceramic (1150 °C during 4 h) shown in Fig. 9 indicates a secondary phase precipitation. The EDX mapping show that this secondary phases are Ti-rich but totally free of the sodium and bismuth. All components of the BNT are present in the main phase. This observation is in good agreement with the $P_{160\text{-aa30\%}}$ green compact EDX mapping (Fig. 10). It can be supposed that this secondary phase is TiO_2. Two hypotheses can be advanced to explain such secondary phase formation. The first one is an incomplete $Ti[OCH(CH_3)_2]_4$ hydrolysis by free water included in $Bi(NO_3)_3{\cdot}5H_2O$. The hydrolysis of the partially reacted powder is then after faster when NaOH is added causing the formation of Ti-rich clusters precipitating in TiO_2 regardless of the BNT perovskite structure. The second hypothesis is a not enough aggressive acetic acid washing, leading in selective leaching of Bi and Na. The excess of titanium precipitate in TiO_2 clusters observed in green compact and then, in titanium oxide during sintering.

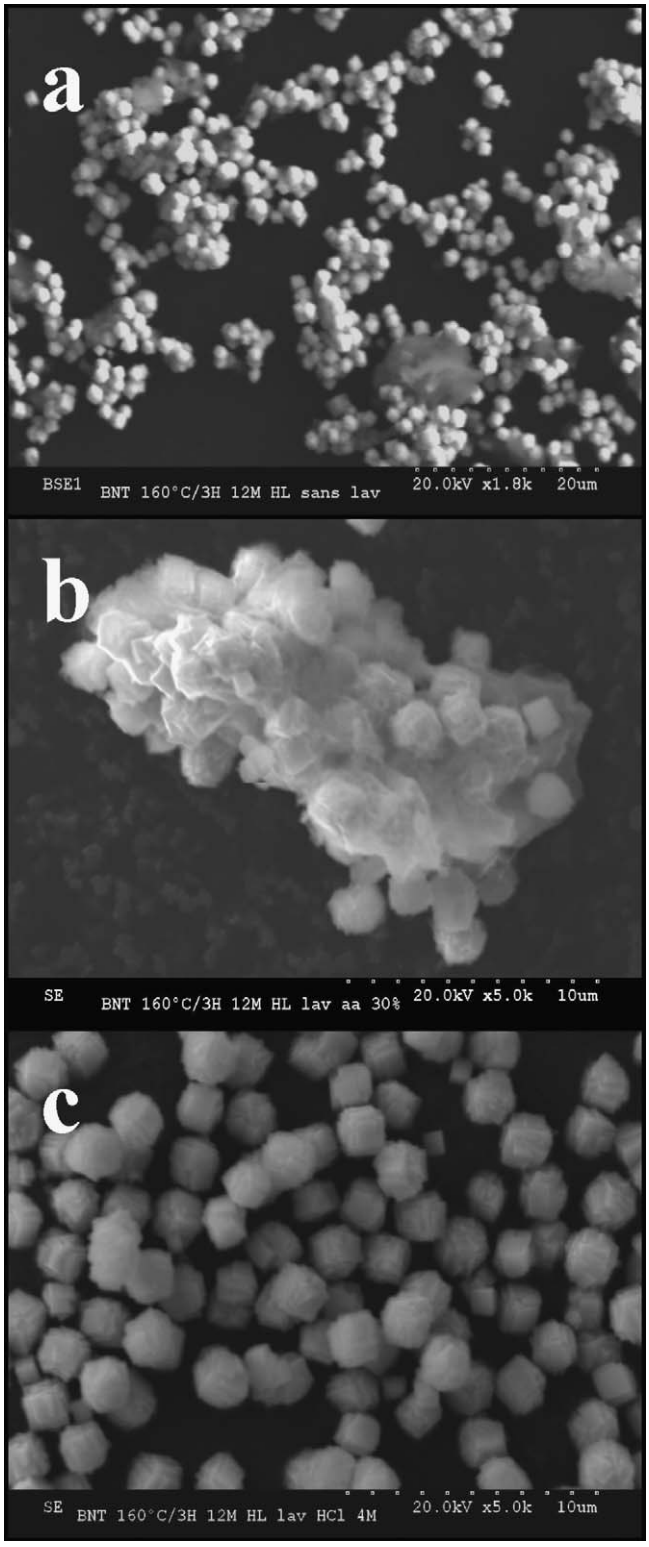

Fig. 8. SEM micrographs of $P_{160\text{-DIw}}$ (a), $P_{160\text{-aa30\%}}$ (b) and $P_{160\text{-HCL4M}}$ (c).

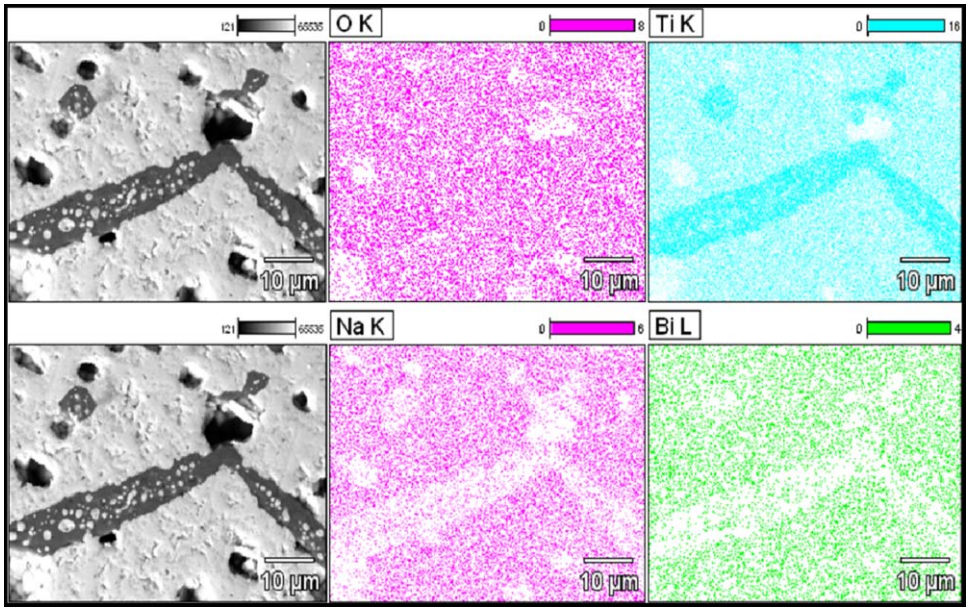

Fig. 9. EDX mapping of the secondary phase observed on the $P_{160\text{-}aa30\%}$ ceramic.

3.2.2. With a 4 M hydrochloric acid solution

The size distribution of $P_{160\text{-}HCl4M}$ is monomodal with a grain size of 2 μm according to the SEM observation (Fig. 8c). No amorphous phase is detected suggesting the 4 M hydrochloric acid solution is sufficient to eliminate it. Two sintering processes have been performed, one at 1050 °C during 4 h and the second one at 1150 °C with the same dwell time.

No secondary phase is detected on $P_{160\text{-}HCl4M}$ sintered piezoceramics (Fig. 11).

The bulk densities were determined by mean of Archimedes method but discrepancies are high regarding to the sample weights. Densification ratios are at least 90%, enough for the samples to be suitably polarized under high electric field.

Fig. 11 shows SEM microstructures of the sintered samples. Some porosity is observed and is due to pull out of grains during the polishing step (Fig. 11a and b). Fig. 11c and d shows SEM observations of cross section samples sintered at 1050 °C and 1150 °C respectively. The first one exhibits fine microstructure, whereas the one sintered at 1150 °C shows a liquid sintering phenomenon leading on a significant grain growth (Fig. 11d) facilitating grain decohesion and pull out. On the contrary, samples sintered at 1050 °C (Fig. 11c) are fine grained indicating that liquid sintering has not yet occurred and no pull out of

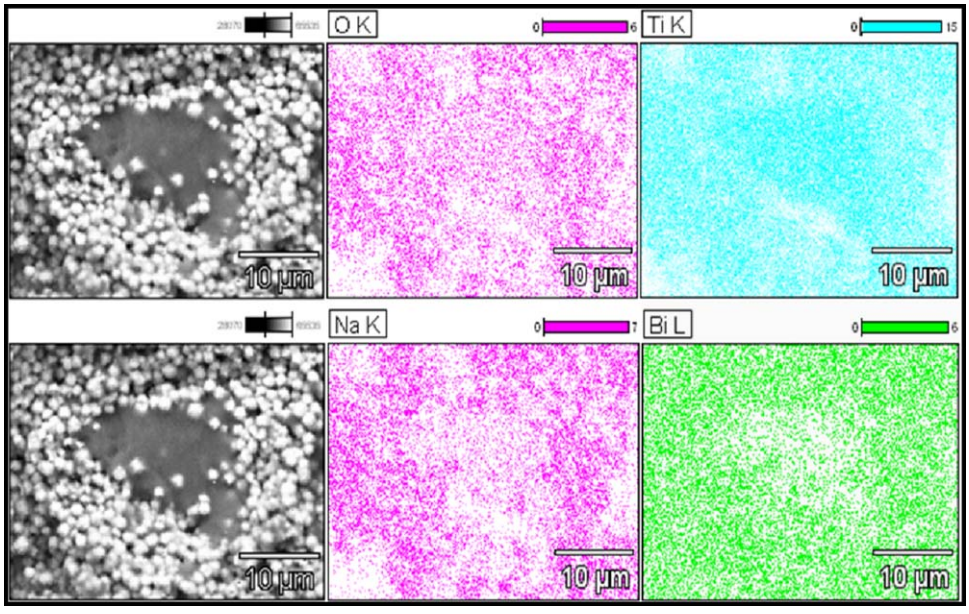

Fig. 10. $P_{160\text{-}aa30\%}$ green compact EDX mapping.

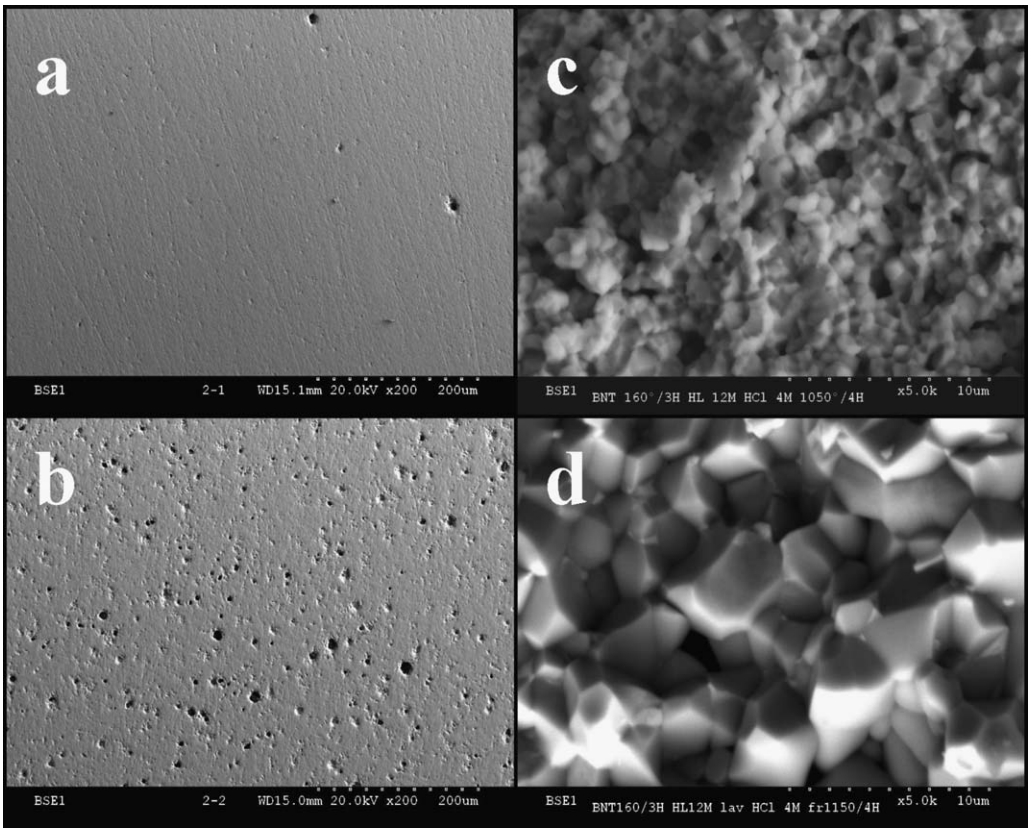

Fig. 11. SEM micrographs of $P_{160\text{-}HCl4M}$ sintered at 1050 °C (a) and 1150 °C (b) during 4 h; cross section SEM micrographs of $P_{160\text{-}HCl4M}$ sintered at 1050 °C (c) and 1150 °C (d) during 4 h.

Table 1
d_{33} charge constants obtained in this study.

Ceramics	d_{33} (pC/N)
$P_{160\text{-}DIw}$ 1150 °C	15
$P_{160\text{-}aa30\%}$ 1150 °C	68
$P_{160\text{-}HCl4M}$ 1050 °C	37
$P_{160\text{-}HCl4M}$ 1150 °C	63

grains appears during sample preparation for SEM observations (Fig. 11a).

The increase of sintering temperature from 1050 °C to 1150 °C favors the occurrence of a liquid assisted grain growth. Large grained piezoceramics are easily polarized and domain wall pinning is lesser. The well known extrinsic effect explains the good piezoelectric properties of these ceramics (Table 1).

4. Conclusion

This study was focused on the BNT powders synthesis by hydrothermal route. A high temperature (265 °C) coupled with a high concentration of NaOH (12 M) favors the TiO_2 nanotubes precipitation. It was then decided to work at lower temperature. For a temperature of 160 °C and a synthesis time of 3 h, single phased BNT powders were successfully synthesized. Nevertheless thermally unstable phases (in minor quantities) were observed in the powder. These phases were shown to be responsible for the emergence of a strong porosity after sintering.

Various washing techniques were then investigated in order to eliminate these unstable phases, by increasing the acidity of the washing solution.

By using the hydrochloric acid and for a sintering temperature of 1150 °C, the hydrothermally synthesized BNT piezoceramics exhibit relatively good densification rate (>90%) and piezoelectric properties (63 pC/N) without any secondary phase.

Acknowledgment

This work was funded by French Government for a PhD thesis program.

References

1. Matsumoto S, Klein A, Maeda R. Development of bidirectional valve-less micropump for liquid. In: *Procedure of IEEE micro electro mechanical system.*; 1998. p. 141–6.
2. Schroth A, Lee L, Matsumoto S, Maeda R. Application of sol gel deposited thin PZT film for actuation of 1D and 2D scanners. *Sensors and Actuators* 1999;**73**:144–52.
3. Chu J, Wang ZJ, Maeda R, Kataota K, Itih T, Suga T. Novel multi-bridge-structured piezoelectric microdevices for scanning force microscopy. *Journal of Vacuum Science and Technology* 2000;**B18**:3604–7.

4. Directive 2002/95/EC of European Parliament and of the Council of 27 January 2003 on Restriction of the Use of Certain Hazardous Substances in Electrical and Electronic Equipment. Official Journal of the European Union.
5. Yasuyoshi S, Hisaaki T, Tashihiko T, Tatsukiko N. Lead-free piezoceramics. *Nature* 2004;**432**(November).
6. Nagata H, Yoshida M, Makiuchi Y, Takenaka T. Large piezoelectric constant and high Curie temperature of lead-free piezoelectric ceramic ternary system based on bismuth sodium titanate–bismuth potassium titanate–barium tinanate near the morphotropic phase boundary. *Japanese Journal of Applied Physics* 2003;**42**:7401–3.
7. Chu BJ, Chen DR, Li GR, Yin QR. Electrical properties of $Na_{1/2}Bi_{1/2}TiO_3$–$BaTiO_3$ ceramics. *Journal of European Ceramic Society* 2002;**22**:2115–21.
8. Xu Q, Chen S, Chen W, Wu S, Zhou J, Sun H, et al. Synthesis and piezoelectric and ferroelectric properties of $(Bi_{0.5}Na_{0.5})_{(1-x)}Ba_xTiO_3$ ceramics. *Materials Chemistry and Physics* 2005;**90**: 111–5.
9. Jing X, Li Y, Yin Q. Hydrothermal synthesis of $Na_{05}Bi_{0.5}TiO_3$ fine powders. *Materials Science and Engineering* 2003;**B99**:506–10.
10. Ma YJ, Cho JH, Lee YH, Kim BI. Hydrothermal synthesis of $(Bi_{1/2}Na_{1/2})TiO_3$ piezoelectric ceramics. *Materials Chemistry and Physics* 2006;**98**:5–8.
11. Kasuga T. Formation of titanium oxide nanotubes using chemical treatments and their characteristic properties. *Thin Solid Films* 2006;**496**: 141–5.
12. Bouaziz R, Papin G. *Phase diagram for ceramists*, vol. III. The American Ceramic Society; 1975 [figure no. 4655].